Int. J. Heat Mass Transfer. Vol. 18, pp. 1113–1118. Pergamon Press 1975. Printed in Great Britain

NONEQUILIBRIUM MERGED STAGNATION SHOCK LAYERS AT HYPERSONIC SPEEDS*

AJAY KUMAR and A. C. JAIN†
Department of Aeronautical Engineering, Indian Institute of Technology, Kanpur, India

(Received 9 September 1974)

Abstract—Nonequilibrium flow calculations are made in the merged stagnation shock layer of a blunt body using full Navier–Stokes equations to describe the flow field. A seven species, six reactions air model is considered. The concept of local similarity is used to reduce the equations to a set of nonlinear coupled ordinary differential equations. This set of equations is solved by the successive accelerated replacement technique. It is found that the present analysis with full Navier–Stokes equations gives higher temperatures in the merged shock layer than thin shock layer analysis. The electron density and mass fractions of N, O and NO are also higher in the present analysis than thin shock layer analysis. Heat transfer to the body surface is discussed and it is seen that the heat-transfer coefficient increases with the decrease in Reynolds number. The results of the present analysis are compared with the other available results.

NOMENCLATURE

C_H, heat-transfer coefficient, $-\bar{q}_w/(\bar{\rho}_\infty \bar{u}_\infty^3/2)$;
C_i, mass fraction of ith species, $\bar{\rho}_i/\bar{\rho}$;
h, dimensionless enthalpy, $\bar{h}/\bar{u}_\infty^2$;
H, total enthalpy;
$(Le)_i$, Lewis number of ith species;
$\bar{M}_i$, mol. wt of ith species;
n_e, effective freestream from body;
N_E, electron density [particles/cm^3];
p, dimensionless pressure, $\bar{p}/\bar{\rho}_\infty \bar{u}_\infty^2$;
p_2, second order term in the expansion for p;
Pr, Prandtl number;
$\bar{q}_w$, heat-transfer rate to the body;
R, universal gas constant;
$\bar{r}_b$, nose radius;
r_e, effective freestream from origin;
$(Re)_\infty$, freestream Reynolds number, $\bar{\rho}_\infty \bar{u}_\infty \bar{r}_b/\bar{\mu}_\infty$;
(Re), Reynolds number, $\bar{\rho}_\infty \bar{u}_\infty \bar{r}_b/\bar{\mu}_0$;
$(Sc)_i$, Schmidt number of ith species;
T, dimensionless temperature, $\bar{T}/\bar{T}_o$;
u, dimensionless tangential velocity, $\bar{u}/\bar{u}_\infty$;
v, dimensionless normal velocity, $\bar{v}/\bar{u}_\infty$;
$\bar{\dot{w}}_i$, mass rate of production of ith species [g/cm^3 s];
$\dot{w}_i$, dimensionless production rate of ith species, $\bar{\dot{w}}_i/(\bar{\rho}_\infty \bar{u}_\infty/\bar{r}_b)$;
η, transformed radial coordinate;
θ, angle between r and axis of symmetry;
μ, dimensionless viscosity coefficient, $\bar{\mu}/\bar{\mu}_0$;
ρ, dimensionless density, $\bar{\rho}/\bar{\rho}_\infty$.

Subscripts
w, wall conditions;
∞, freestream conditions;
0, freestream stagnation conditions.

Superscript
$(\bar{\ })$, dimensional quantities.

*This work was supported by the Vikram Sarabhai Space Centre, Trivandrum, India under a project entitled 'Hypersonic Viscous Flow Around Axisymmetric Bodies at High Altitudes'.

†Presently on leave at Marshall Space Flight Center, Huntsville, Ala., U.S.A.

1. INTRODUCTION

WHEN a space vehicle re-enters into the earth's atmosphere, the temperatures occuring near the body are very high. The air in the surrounding flow field dissociates and ionizes because of this severe aerodynamic heating. In case of a blunt body, the electrons are generated mainly in the shock layer and the number density of electrons is expected to be maximum in the stagnation region. The mole fraction of such electrons is too small to significantly affect the thermodynamic and transport properties but this degree of ionization is large in terms of its influence on electrical conductivity and may lead to communication blackout. To determine the interaction of an electromagnetic signal and a re-entry vehicle, it is essential to predict accurately the ionization level in the shock layer. This, in turn, requires an accurate flow field model taking into account the finite rate chemistry.

The previous investigations [1, 2] of the nonequilibrium ionization in the shock layer of blunt bodies are based on the inviscid flow model which cannot represent the flow field at high altitudes and leads to large over prediction of the ionization level. Chung, Holt and Liu [3] considered the nonequilibrium viscous shock layer in the stagnation region for a binary dissociating gas. Later, Lee and Zierten [4] made calculations for nonequilibrium merged layer ionization in the stagnation region of a blunt body using an approximate model. In their analysis, they solved the species conservation equations for a multi-component gas mixture assuming that the flow properties are given by frozen flow solutions. This assumption decouples the species conservation equations from the fluid dynamic equations, thus simplifying the analysis to a great extent. Blottner [5] also investigated the nonequilibrium flow in the stagnation region by considering thin viscous shock layer regime and using Rankine–Hugonoit relations to obtain the flow conditions at the edge of the shock layer. Dellinger [6] improved the analysis of Lee and Zierten [4] by making simultaneous calculations of the ionization and the neutral gas flow field in the merged stagnation shock layer under the thin shock layer assumption. He found that Lee and Zierten's analysis over predicted the electron density in the shock layer. Recently, Adimurthy and Jain [7] investigated in detail the stagnation point flow and concluded that the thin shock layer assumption is not valid at high altitudes where the Reynolds number is very low making the shock layer thickness comparable to the body radius. They suggested that at such low (Re), full Navier–Stokes equations should be used to describe the flow.

In the present analysis, no thin shock layer assumption is made. The flow field in the stagnation region of the blunt body is described by the full Navier–Stokes equations. The nonequilibrium calculations are made for a seven species, six reactions air model. The species considered are N_2, O_2, NO, N, O, NO^+ and e^-. For air dissociation and ionization, the rate expressions recommended by Wray [8] are adopted. Pr and (Le) are taken to be 0·75 and 1·4 respectively, for neutral species. Ambipolar diffusion is assumed for the electrons and ions so that their diffusion coefficients are twice that of the neutral species. Nonequilibrium merged stagnation solutions are obtained for a multicomponent gas mixture using the concept of local similarity which reduces the equations to a set of nonlinear coupled ordinary differential equations. This set of equations is solved for a fully catalytic wall using the successive accelerated replacement technique.

The results are compared with the theoretical results of Lee and Zierten [4] and Dellinger [6]. It is found that the present analysis with full Navier–Stokes equations gives higher temperatures in the shock layer than thin shock layer analysis. Further, although the analysis of Lee and Zierten [4] predicts higher electron density, the over prediction is not as large as estimated by Dellinger [6]. Results are also obtained for varying nose radius at 90 km altitude. Heat-transfer coefficient is compared with the results of Cheng [9] and Blottner [5].

2. FORMULATION OF THE PROBLEM

Governing equations

The nonlinear, coupled ordinary differential equations governing the flow of a multicomponent gas in the merged stagnation shock layer of an axisymmetric body can be obtained from the full Navier–Stokes equations using the concept of local similarity as

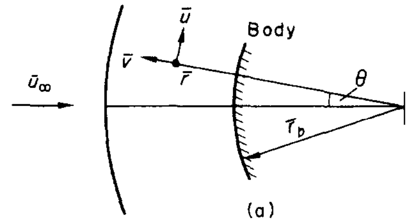

FIG. 1(a). Dimensional coordinate system.

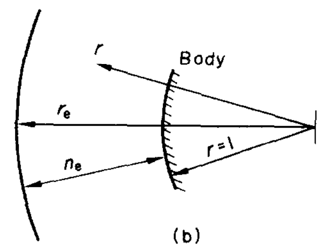

FIG. 1(b). Dimensionless coordinate system.

discussed by Kao [10]. The dimensional and nondimensional coordinate systems are shown in Fig. 1(a) and (b) respectively. The dimensionless equations in stagnation region are as given below.

$$\frac{\rho'}{\rho}=\frac{n_e}{(1+n_e\eta)v}\left[-2(u+v)-\frac{(1+n_e\eta)}{n_e}v'\right] \tag{1}$$

$$\frac{\rho v C_i'}{n_e}=\dot{w}_i+\frac{1}{(1+n_e\eta)(Re)(Sc)_i}\times\left[\left\{2\mu+\mu'\frac{(1+n_e\eta)}{n_e}\right\}\frac{C_i'}{n_e}+\frac{\mu(1+n_e\eta)}{n_e^2}C_i''\right] \tag{2}$$

$$\frac{u''}{n_e^2}=\frac{(u+v)}{(1+n_e\eta)}\left[\frac{8}{3(1+n_e\eta)}+\frac{\mu'}{\mu n_e}+\frac{(Re)\rho u}{\mu}\right]+\frac{(Re)\rho v u'}{\mu n_e}+\frac{v'}{3n_e(1+n_e\eta)}-\frac{u'}{n_e}\left(\frac{2}{1+n_e\eta}+\frac{\mu'}{\mu n_e}\right)+\frac{2p_2(Re)}{(1+n_e\eta)} \tag{3}$$

$$\frac{p_2'}{n_e}=-\frac{p'}{n_e}+\frac{\rho u(u+v)}{(1+n_e\eta)} \tag{4}$$

$$\frac{v''}{n_e^2}=\frac{3(Re)}{4\mu}\left(\frac{p'+\rho v v'}{n_e}\right)-\frac{v'}{n_e}\left(\frac{2}{1+n_e\eta}+\frac{\mu'}{\mu n_e}\right)-\frac{u'}{2n_e(1+n_e\eta)}+\frac{u+v}{(1+n_e\eta)}\left[\frac{7}{2(1+n_e\eta)}+\frac{\mu'}{\mu n_e}\right] \tag{5}$$

$$\begin{aligned}\frac{(Re)\rho v h'}{n_e}&=\frac{(Re)vp'}{n_e}+\frac{2\mu v'^2}{n_e^2}+\frac{4\mu(u+v)^2}{(1+n_e\eta)^2}-\frac{2\mu}{3(1+n_e\eta)^2}\left[\frac{(1+n_e\eta)v'}{n_e}+2(u+v)\right]^2\\&+\frac{1}{Pr(1+n_e\eta)}\left[\left\{2\mu+\frac{\mu'(1+n_e\eta)}{n_e}\right\}\frac{h'}{n_e}+\frac{\mu(1+n_e\eta)h''}{n_e^2}\right]\\&+\frac{1}{Pr(1+n_e\eta)}\left[\left\{2\mu+\frac{\mu'(1+n_e\eta)}{n_e}\right\}\sum_i\left\{h_i((Le)_i-1)\frac{C_i'}{n_e}\right\}\right.\\&\left.+\mu(1+n_e\eta)\sum_i\left\{((Le)_i-1)\left(\frac{h_i'C_i'+h_iC_i''}{n_e^2}\right)\right\}\right]\end{aligned} \tag{6}$$

$$p = \frac{\rho R T \bar{T}_o}{\bar{u}_\infty^2} \sum_i \frac{C_i}{\bar{M}_i} \tag{7}$$

$$\mu = \mu(T). \tag{8}$$

Here, a prime denotes differentiation with respect to η where $\eta = (r-1)/(r_e-1)$ and $(r_e-1) = n_e$. This transformation keeps the body at $\eta = 0$ and the freestream at $\eta = 1$.

The boundary conditions with fully catalytic wall condition are

(i) On the body surface ($\eta = 0$)

$$\begin{aligned} u = v = 0, \quad T = T_w, \quad C_{N_2} = 0{\cdot}79, \quad C_{O_2} = 0{\cdot}21, \\ C_{NO} = C_N = C_O = C_{NO^+} = C_{e^-} = 0. \end{aligned} \tag{9}$$

(ii) In the freestream ($\eta = 1$)

$$\begin{aligned} u = 1, \quad v = -1, \quad \rho = 1, \quad T = T_\infty, \quad p_2 = 0 \\ C_{N_2} = 0{\cdot}79, \quad C_{O_2} = 0{\cdot}21, \\ C_{NO} = C_N = C_O = C_{NO^+} = C_{e^-} = 0. \end{aligned} \tag{10}$$

Air Chemistry

The nonequilibrium calculations are made for a seven species, six reactions air model. The species considered are N_2, O_2, NO, N, O, NO^+ and e^-. Of these species, NO has the lowest ionization energy and is first to produce electrons as the temperature is increased. Practically all the electrons which appear in the air at intermediate temperatures come from the ionization of NO. The reactions considered are given below.

$$O_2 + M + 5{\cdot}1\,\text{eV} \underset{k_{r1}}{\overset{k_{f1}}{\rightleftarrows}} O + O + M$$

$$N_2 + M + 9{\cdot}8\,\text{eV} \underset{k_{r2}}{\overset{k_{f2}}{\rightleftarrows}} N + N + M$$

$$NO + M + 6{\cdot}5\,\text{eV} \underset{k_{r3}}{\overset{k_{f3}}{\rightleftarrows}} N + O + M$$

$$NO + O + 1{\cdot}4\,\text{eV} \underset{k_{r4}}{\overset{k_{f4}}{\rightleftarrows}} O_2 + N$$

$$N_2 + O + 3{\cdot}3\,\text{eV} \underset{k_{r5}}{\overset{k_{f5}}{\rightleftarrows}} NO + N$$

$$N + O + 2{\cdot}8\,\text{eV} \underset{k_{r6}}{\overset{k_{f6}}{\rightleftarrows}} NO^+ + e^-$$

Here 'M' is the catalytic species. k_{fj} and k_{rj} are the temperature dependent forward and reverse reaction rates respectively for the jth reaction. Reactions leading to electronically excited species are not considered.

For air dissociation and ionization, the rate expressions recommended by Wray [8] are taken. The mass production rates for various species can be obtained using these reaction rates. The enthalpy of air is calculated assuming that molecules in the shock layer possess full rotational as well as vibrational degrees of freedom and that excitation of electronic states of the atoms and molecules is neglected.

3. METHOD OF SOLUTION

Equations (1)–(8) constitute a set of nonlinear, coupled ordinary differential equations with boundary conditions given by (9) and (10). These equations are integrated by a finite difference method known as successive accelerated replacement method. The method is successfully used earlier by Dellinger [6] and by Adimurthy and Jain [7]. Successive accelerated replacement technique is applied only to second order equations, while the first order equations are solved by direct numerical quadrature. The details and various advantages of the method over other methods are given in [6].

Species conservation equation is used to calculate the mass fractions of O_2, NO, N, O and NO^+. Knowing the mass fraction of NO^+, the condition of charge neutrality gives the electron density in the merged shock layer. Mass fraction of N_2 is obtained using

$$\sum_i C_i = 1.$$

4. RESULTS AND DISCUSSION

The results of the present analysis are compared with that of Dellinger [6] and Lee and Zierten [4]. The same viscosity law is used as taken by these authors. The nonequilibrium calculations are also made at an altitude of 90 km with $\bar{u}_\infty = 7000$ m/s and varying body radius. The viscosity is assumed to vary as square root of temperature for this case.

Figures 2–4 compare the present results with that of Dellinger [6] at $Re_\infty = 920$. Electron density profiles are plotted in Fig. 3. Present calculations are made with reaction rates recommended by Wray [8] and also with reaction rates used by Dellinger [6]. It is seen from Fig. 3 that the electron density values obtained by Dellinger [6] are smaller than the present values in the entire merged shock layer. This can be explained by examining the corresponding flow field properties in Fig. 2 which shows that Dellinger's analysis predicts lower temperatures in the merged shock layer. This difference in temperature gives rise to the observed difference in the electron density because of its effect on the chemical reaction rates. Due to higher temperatures, the dissociation of nitrogen and oxygen is more in the present analysis giving higher mass fractions of other species plotted in Fig. 4.

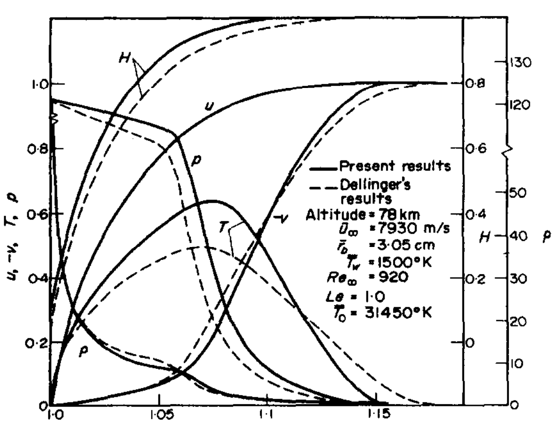

FIG. 2. Comparison of u, $-v$, T, p, ρ with the results of Dellinger.

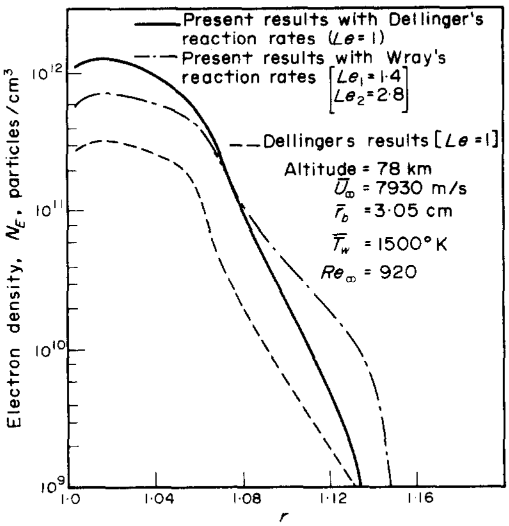

FIG. 3. Comparison of electron density with the results of Dellinger.

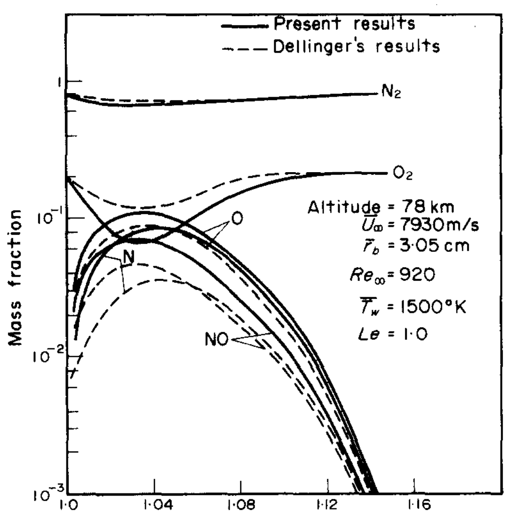

FIG. 4. Comparison of species mass fractions with the results of Dellinger.

Figure 2 further shows that while there is small difference in total enthalpy, the difference in temperature is relatively large due to the difference in the normal velocity component. This is due to the fact that for a given total enthalpy, even a small change in normal velocity results in a larger change in the static enthalpy since it is proportional to the square of the normal velocity.

Figures 5–7 compare the results of Lee and Zierten [4] and Dellinger [6] with the present results at $(Re)_\infty = 814$. Figure 5 shows that although Lee and Zierten [4] over predicted the electron density, the difference is not as large as obtained by Dellinger. In Figure 6, the chemical production rates of N, O and e^- are compared. It is seen that the present analysis gives lower production rates for O and e^- and higher production rate for N. Mass fractions of various species are plotted in Figure 7 and are compared with the results of Lee and Zierten [4]. Present analysis gives higher mass fractions of N and NO and lower mass fraction of O.

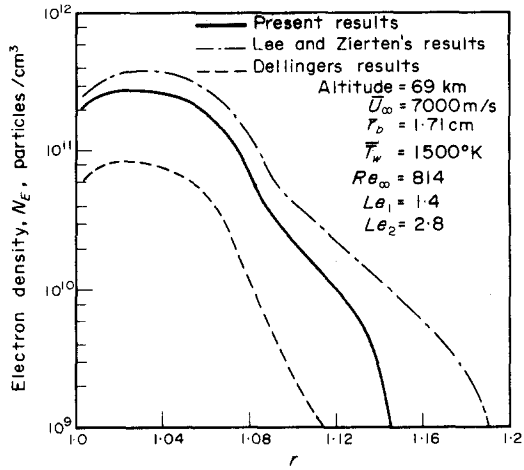

FIG. 5. Comparison of electron density with the results of Dellinger and Lee and Zierten.

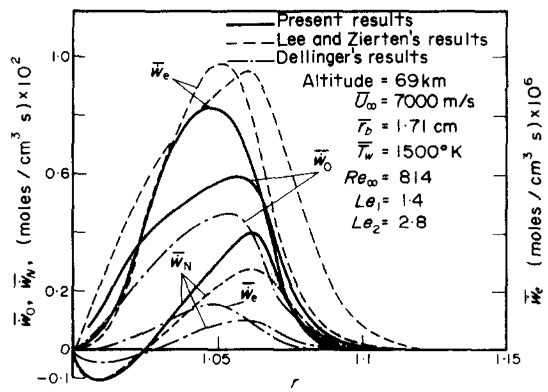

FIG. 6. Comparison of species production rates with the results of Dellinger and Lee and Zierten.

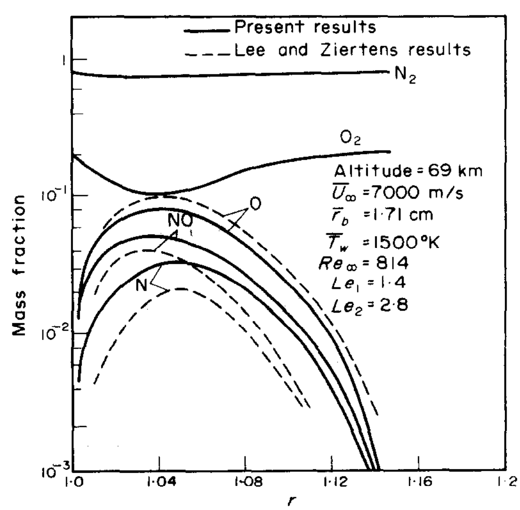

FIG. 7. Comparison of species mass fractions with the results of Lee and Zierten.

Calculations for stagnation point heat-transfer coefficient C_H are made for varying body radius at an altitude of 90 km with freestream velocity equal to 7000 m/s. The results of the present calculations are compared with that of Cheng [9] and Blottner [5] in Fig. 8. Cheng's results are for binary mixture of diatomic molecules and dissociating atoms while the present results and Blottner's results are for a complete

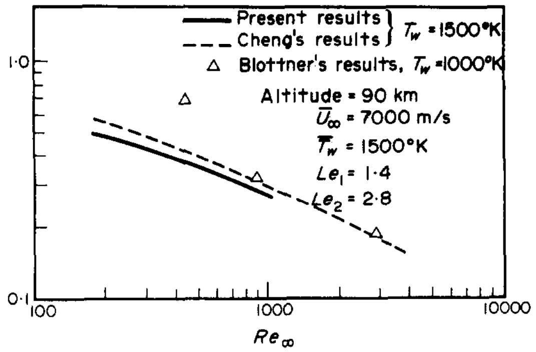

FIG. 8. Comparison of heat-transfer coefficient.

air model. The results of Blottner are not valid at low (Re) because he obtained the flow conditions at the edge of the shock layer from Rankine–Hugonoit relations. Blottner made calculations with the wall temperature equal to 1000°K while Cheng took it as 1500°K. Since the value of C_H depends on the wall temperature, the agreement of the results of Blottner with Cheng may not be as good as is seen in Fig. 8 even at higher (Re). Present analysis predicts slightly lower values of C_H than Cheng and the difference increases with decreasing (Re). This is because Cheng's two thin-layer model becomes more and more inaccurate as the (Re) decreases.

REFERENCES

1. J. C. Hall, A. Q. Eschenroeder and P. V. Marrone, Blunt-nose inviscid air flows with coupled nonequilibrium processes, *J. Aerospace Sci.* **29**, 1038 (1962).
2. D. Ellington, Approximate method for hypersonic non-equilibrium blunt body air flows, *AIAA Jl* **1**, 1901 (1963).
3. P. M. Chung, J. F. Holt and S. W. Liu, Merged stagnation shock layer of a nonequilibrium dissociating gas, *AIAA Jl* **6**, 2372 (1968).
4. R. H. C. Lee and T. A. Zierten, Merged layer ionization in the stagnation region of a blunt body, *Proceedings of the 1967 Heat Transfer and Fluid Mechanics Institute*, pp. 452–468, Stanford University Press, Stanford, Calif. (1967).
5. F. G. Blottner, Viscous shock layer at the stagnation point with nonequilibrium air chemistry, *AIAA Jl* **7**, 2281 (1969).
6. T. C. Dellinger, Computation of nonequilibrium merged stagnation shock layers by successive accelerated replacement, *AIAA Jl* **9**, 262 (1971).
7. A. C. Jain and V. Adimurthy, Hypersonic merged stagnation shock layers—Parts I and II, *AIAA Jl* **12**, 342 (1974).
8. K. L. Wray, Chemical kinetics of high temperature air, in *Hypersonic Flow Research*, edited by F. R. Riddell, pp. 181–204. Academic Press, New York (1962).
9. H. K. Cheng, The blunt body problem in hypersonic flow at low Reynolds number, Cornell Aeronautical Laboratory Report No. AF 1285-A-10 (1963).
10. H. C. Kao, Hypersonic viscous flow near the stagnation streamline of a blunt body—I. A test of local similarity, *AIAA Jl* **2**, 1892 (1964).

COUCHE DE CHOC D'ARRET EN NON EQUILIBRE AUX VITESSES HYPERSONIQUES

Résumé—Les calculs de l'écoulement en non équilibre effectués dans la couche de choc d'arrêt d'un solide émoussé utilisent les équations de Navier–Stokes complètes pour décrire le champ du mouvement. Un modèle à sept composantes et six réactions est considéré pour l'air. La notion de similitude locale est utilisée afin de réduire les équations à un système d'équations différentielles ordinaires non-linéaires couplées. Ce système d'équations est résolu par une technique de relaxations successives accélérés. On trouve que la présente analyse qui retient les équations de Navier–Stokes complètes fournit des températures plus élevées dans la surface de choc diffuse que ne donne l'analyse des couches de choc minces. La densité électronique et les fractions massiques de N, O et NO sont également plus élevées dans la présente analyse que dans l'analyse des couches de choc minces. Le transfert de chaleur à la surface du solide est examiné et il apparait que le coefficient de transfert thermique augmente lorsque le nombre de Reynolds diminue. Les résultats de la présente analyse sont comparés aux autres résultats disponibles.

VERMISCHTE STAUGEBIETS-STOSSSCHICHTEN IM NICHTGLEICHGEWICHT BEI HYPERSONISCHEN GESCHWINDIGKEITEN

Zusammenfassung—Es wird die Strömung bei Nichtgleichgewicht im Bereich vermischter Stoßschichten im Staugebiet eines stumpfen Körpers berechnet. Zur Beschreibung des Strömungsfeldes werden die vollständigen Navier–Stokes-Gleichungen verwendet; es wird ein 7-Komponenten Luftmodell mit 6 Reaktionen zugrundegelegt. Mit Hilfe des Konzepts der lokalen Ähnlichkeit werden die Gleichungen auf ein System nichtlinear gekoppelter, gewöhnlicher Differentialgleichungen reduziert. Es zeigt sich, daß die vorliegende Untersuchung mit den vollständigen Navier–Stokes-Gleichungen höhere Temperaturen in der vermischten Stoßschicht ergibt als nach der bisherigen Näherung durch das dünne Stoßschichtmodell. Ebenso ergeben sich für die Elektronendichte und die Massenanteile von N, O und NO höhere Werte. Der Wärmeübergang an den Körper wird diskutiert, wobei sich eine Zunahme des Wärmeübergangskoeffizienten mit abnehmender Reynolds-Zahl ergibt. Die Ergebnisse werden mit anderen vorliegenden Resultaten verglichen.

НЕРАВНОВЕСНЫЕ УДАРНЫЕ СЛОИ ПРИ ГИПЕРЗВУКОВЫХ СКОРОСТЯХ

Аннотация — С пошощью полных уравнений Навье-Стокса выполнен расчет неравновесного течения в ударном слое вблизи точки торможения тупого тела. Анализ проведен на воздухе. Понятие локального подобия использовано для приведения уравнений к системе обычных нелинейных дифференциальных уравнений, которые решаются методом последовательной замены переменных. Найдено, что при использовании полных уравнений Навье–Стокса получаются более высокие значения температур для указанных ударных слоев, чем при анализе тонких ударных слоев. Также более высокими получаются значения плотности электронов и относительного массового содержания N, O и NO. Рассмотрен перенос тепла к поверхности тела и показано, что с уменьшением числа Рейнольдса коэффициент теплообмена возрастает.

Проведено сравнение результатов данного анализа с другими имеющимися результатами.